IMPACT OF IRON CONTAMINATION IN MULTICRYSTALLINE SILICON SOLAR CELLS: ORIGINS, CHEMICAL STATES, AND DEVICE IMPACTS

Tonio Buonassisi[1†], Matthias Heuer[1,2], Andrei A. Istratov[1], Matthew A. Marcus[3], Ralf Jonczyk[4], Barry Lai[5], Zhonghou Cai[5], Roland Schindler[6], Eicke R. Weber[1]

[1]University of California at Berkeley and Lawrence Berkeley National Laboratory, Berkeley, USA; [2]University of Leipzig, Leipzig, Germany; [3]Advanced Light Source, Lawrence Berkeley National Laboratory, Berkeley, USA; [4]GE Energy, Newark, USA; [5]Advanced Photon Source, Argonne National Laboratory, Argonne, USA; [6]Fraunhofer Institute for Solar Energy Systems, Freiburg, Germany; † Corresponding author: T. Buonassisi, buonassisi@alumni.nd.edu.

ABSTRACT: Synchrotron-based microprobe techniques have been applied to study the distribution, size, chemical state, and recombination activity of Fe clusters in two types of mc-Si materials: block cast mc-Si, and AstroPower Silicon Film™ sheet material. In sheet material, high concentrations of metals were found at recombination-active, micron-sized intragranular clusters consisting of micron and sub-micron sized particles. In addition, Fe nanoparticles were located in densities of ~2×10^7 cm^{-2} along recombination-active grain boundaries. In cast mc-Si, two types of particles were identified at grain boundaries: (1) micron-sized oxidized Fe particles accompanied by other metals (Cr, Mn, Ca, Ti), and (2) a higher number of sub-micron $FeSi_2$ precipitates that exhibited a preferred orientation along the crystal growth direction. In both materials, it is believed that the larger Fe clusters are inclusions of foreign particles, from which Fe dissolves in the melt to form the smaller $FeSi_2$ nanoprecipitates, which by virtue of their more homogeneous distribution are deemed more dangerous to solar cell device performance. Based on this understanding, strategies proposed to reduce the impact of Fe on mc-Si electrical properties include gettering, passivation, and limiting the dissolution of foreign Fe-rich particles in the melt.
Keywords: lifetime-limiting defects, advanced characterization tools, impurities

1 INTRODUCTION

Iron is the most abundant metallic impurity in multicrystalline silicon (mc-Si) solar cell material, often found in concentrations up to $10^{14\text{-}16}$ Fe cm^{-3} [1, 2]. It is well-known that for single-crystalline silicon, only 2×10^{12} cm^{-3} of interstitial iron or 2×10^{13} cm^{-3} of iron-boron pairs is sufficient to decrease the minority carrier diffusion length to 50 µm ($\tau \sim 1$ µs), unacceptable for most cost-effective PV devices [3]. Yet despite Fe concentrations orders of magnitude higher, mc-Si materials regularly achieve minority carrier diffusion lengths in excess of 100 µm. In mc-Si, the key to understanding the impact of Fe lies not in its absolute concentration, but in its distribution and chemical state.

Up to now, little has been known about these properties of Fe in mc-Si because a technique with appropriate sensitivity and scanning volume was not available to regularly detect and characterize inhomogeneously-distributed, nanometer-sized metal clusters embedded within the silicon matrix. Now, with the development of synchrotron-based x-ray microprobe techniques, one can determine the recombination activity, elemental composition, size, and chemical state of metal precipitates a few tens of nanometers in diameter, with sub-micron spatial resolution [4]. Herein, we apply synchrotron-based microprobe techniques to characterize the distribution, size, chemical state, and recombination activity of iron-rich clusters in AstroPower Silicon Film™ sheet material and block cast mc-Si. These investigations provide insights about the origins of these particles, as well as strategies to reduce their impact on solar cell devices.

2 DESCRIPTION OF TECHNIQUES

X-ray microprobe studies typically commence with a large-area (several mm^2) X-ray beam induced current (XBIC) map, which effectively measures the minority carrier recombination activity. For the samples analyzed in this study, the XBIC signal was collected by a 20 nm thick Al diode deposited after thoroughly cleaning and slightly etching the sample surfaces in a mixture of $HF:HNO_3$. In regions of high recombination activity identified by low XBIC signal, higher-resolution X-ray fluorescence microscopy (µ-XRF) maps can determine the presence of nanometer-sized metal clusters in silicon [4, 5]. Synchrotron-based µ-XRF has the advantage of high fluxes of $10^{9\text{-}12}$ photons/s^{-1} and small spot sizes with diameters ranging from 7 down to 0.2 µm. By optimizing all parameters, near-surface Fe clusters with radii $\geq$16±3 nm are detectable within 1s accumulation time. For particles located in the bulk, the XRF signal intensity decreases according to an element-specific attenuation length, which increases with atomic number Z, e.g. 36 µm for Fe and 70 µm for Cu.

Once a cluster is located by µ-XRF, X-ray absorption microspectroscopy (µ-XAS) can measure the X-ray absorption spectrum of the impurity species, which is unique to its bonding structure and chemical state [5]. By comparison with standard material, a positive identification of the chemical state of the impurity atoms within the cluster can be obtained.

The microprobe tools used in this study include beamlines 10.3.1 and 10.3.2 [15] of the Advanced Light Source (ALS) at Lawrence Berkeley National Laboratory, in addition to high-resolution studies performed at beamline 2-ID-D [16] of the Advanced Photon Source (APS) at Argonne National Laboratory.

3 SHEET MATERIAL

3.1 Experimental Results

One piece of sheet material was aluminum gettered

at 800°C for 4 hours to promote the dissolution of metal clusters. A typical XBIC image from this sample is shown in Fig. 1a (dark = low XBIC signal). Features of interest include (a) highly recombination-active grain boundaries and (b) localized regions of high recombination activity within the grains, with a recovery of minority carrier diffusion length in between.

High-resolution µ-XRF mapping of these two distinct low-lifetime features reveals the presence of Fe distributed in different ways. Firstly, the grain boundaries contain a multitude of nanometer-sized Fe particles, as can be seen from Fig. 1b. A comparison of the signal strength with that from standard material revealed an estimate for the assumed-spherical particle radii to be ~23±5 nm. Given the attenuation length of the Fe fluorescence signal, the density of these Fe nanoparticles along the grain boundary was estimated to be ~2×10^7 cm^{-2}, consistent with etching experiments by Lu *et al*. [14]. The regions of decreased XBIC signal within the grains are found to contain Fe arranged in micron-sized clusters consisting of multiple smaller particles. The average size of the Fe particles within these large clusters is notably higher than the grain boundary nanoprecipitates, as evidenced by a log scale on the µ-XRF map in Fig. 1c. In addition to Fe, some Cr is evident from the µ-XRF point spectrum. µ-XAS indicates the chemical state of the Fe in both types of defects is most likely to be in the form of an iron silicide, as shown in Fig. 1d.

In as-grown material, intragranular defect clusters are accompanied by substantial amounts of chromium and nickel, in addition to iron (Fig. 2a). These metals are present in metal silicide form (Fig. 2b). The relative concentrations of these elements, determined by the heights of the fluorescence peaks shown in Fig. 2a, matches those of certain stainless steels, suggesting these clusters originated from foreign stainless steel particles the feedstock. In addition, the relative Cr, Ni, and Fe concentrations in these clusters match those obtained via neutron activation analysis on this material [2], suggesting that these clusters account for a large fraction of the total metal content in this sample.

3.2 Discussion

The concentration of metallic impurities within large clusters is widely believed to be preferable over their being distributed as point defects throughout the wafer [7, 8]. In this manner, sheet material can achieve relatively high diffusion lengths while incorporating large absolute quantities of metallic impurities. Nevertheless, metals associated with these intragranular clusters bear important consequence on material performance via two mechanisms:

(a) Recombination at the intragranular clusters: Provided the grain size is large, the spatial density of these intragranular clusters will limit the intragranular diffusion length. This has been both predicted theoretically [7] and observed experimentally [4] to be the case. It is thus preferable that the spatial density of these clusters within one diffusion length of the pn junction be as low as possible.

(b) Metal clusters as source for distributed impurities: µ-XAS data indicates Fe is present in the finished crystal as $FeSi_2$. Since the total time the feedstock is melted is rather short for this process, it is unlikely that iron was originally present in oxidized particles, lest it be evident as such in the final crystal. More likely, these metals were in a metallic state right before crystal growth, which means atoms from these clusters could easily dissolve in the silicon melt. These dissolved metal atoms can easily contaminate nearby structural defects, such as grain boundaries. This is the likely origin of the $FeSi_2$ nanoprecipitates detected at the grain boundaries, where XBIC indicates they have a high recombination activity.

Recent data from illuminated lock-in thermography (ILT) measurements on mc-Si material indicate that recombination at grain boundaries is a major power loss mechanism for solar cells in illuminated conditions [9]. In light of this fact, it is of extreme interest to (a) limit grain boundary surface area near the pn-junction, and to (b) limit the Fe contamination of these grain boundaries by restricting the dissolution of the large intragranular metal clusters. Further investigations into the distribution and recombination activity of metal clusters at grain boundaries in response to gettering and passivation treatments are needed.

4 CAST MC-SI MATERIAL

4.1 Experimental Results

A cast mc-Si wafer cut vertically from the ingot (i.e. perpendicular to the solidification front) was processed into solar cells at Fraunhofer Institute for Solar Energy Systems in Freiburg, Germany. Material within this solar cell from near the bottom of the ingot was selected for microprobe analysis because of its lower diffusion length. The ARC and metallization was removed by chemical etching, and an Al diode was deposited for XBIC analysis, as described in Sec. 2.

Grain boundaries with high recombination activity are evident in XBIC maps, such as that in Fig. 3a. µ-XRF and µ-XAS scans of these grain boundaries reveal two types of Fe-rich cluster, which can be seen as spots of relatively higher and lower Fe XRF counts in the µ-XRF map of Fig. 3b. The characteristics of these two types of Fe-rich clusters are detailed below:

Type 1: While each Type 1 Fe-rich particle has a lower Fe XRF count rate, they are the more numerous of the two types. µ-XAS scans show a clear signal of $FeSi_2$ at these locations (Fig. 3c), and µ-XRF point scans show only Fe above the detection limit. High-resolution µ-XRF scans determined an elongation of these particles along the grain boundary and crystal growth direction; dimensions are typically 200-290 nm diameter across (parallel to the solidification front) and 550-775 nm diameter vertically (normal to the solidification front, parallel to the grain boundary and crystal growth directions). Note that the X-ray beam spot size is approximately 200 nm in diameter, thus the width of these particles may actually be smaller than 200 nm.

Type 2: These particles are less frequently found, yet they contain large amounts of iron, and to a lesser extent, other impurities such as Mn, Cr, Ti, and Ca. µ-XAS scans show that the Fe in these particles is in an oxidized form (Fe_2O_3, Fig. 3d). High-resolution µ-XRF scans show that these particles are typically 1250-1500

nm across and 900-1200 nm in the vertical direction, i.e. *not* elongated along the crystal growth direction.

4.2 Discussion

The origins of these particles appear to be similar to the case of sheet material, with a few key differences: Firstly, the large Type 2 clusters are oxidized. It is rather unusual and unexpected to find oxidized Fe particles in silicon, since they are not thermodynamically favored to form. Silicon, which has a higher binding energy to oxygen than iron, will be a strongly reducing atmosphere for any oxidized iron. It is thus more likely, given the oxidized chemical state and presence with other metals reminiscent of stainless steels or ceramics, that the Type 2 particles are the remnants of foreign particles included in the melt, from the feedstock or possibly from the crucible walls, as was suggested by Rinio *et al.* [13]. Because the cast mc-Si process maintains a liquid melt for many hours, these oxidized particles should survive only a rather short time before complete dissolution in the melt, i.e. one would expect to find them only towards the bottom of the ingot.

However, as these foreign particles are dissolving in the melt, they most certainly can increase the Fe content of the melt considerably. To reduce the Fe content in the melt and avoid supersaturation, atomically dissolved Fe is likely to precipitate in the form of $FeSi_2$.

Iron silicide clusters such as the Type 1 particles (as well as those below the current detection limit of the µ-XRF technique) are likely to make the greatest contribution to the recombination activity of grain boundaries in this material, due to their higher spatial density following from arguments presented in Sec. 3.2. As can be seen from the µ-XRF map in Fig. 3b, the distances between Type 1 particles can be as small as 20 µm, which is predicted to severely limit the minority carrier diffusion length [10]. As shown by ILT and described in Sec. 3.2, recombination at grain boundaries may make a large contribution to the total power loss of an illuminated mc-Si solar cell. It is thus of interest to identify means of reducing the impact of these defects on minority carrier diffusion length. Three possibilities are identified and discussed forthwith: (a) gettering existing Type 1 defects, (b) passivating Type 1 defects, and (c) limiting the dissolution of Type 2 particles in the melt.

(a) Gettering has shown mixed results when applied to mc-Si materials [11]. This is believed to be due to the fact that large Fe-rich particles do not fully dissolve during normal gettering sequences, because of the relatively low diffusivity and solubility of Fe in Si [7]. Thus, when the gettering sequence ends, there are still dissolving Fe-rich particles, and thus there will still be Fe dissolved within the silicon bulk at its solubility limit. A slow cool is thus advised at the end of the gettering step, to allow for the dissolved Fe to diffuse to the most energetically favorable sites, thus giving Ostwald ripening a chance to occur. If cooling from the high gettering temperature occurs too quickly, then supersaturated Fe dissolved in the bulk will be forced to precipitate at the nearest available precipitation site or to remain dissolved within the grains as point defects, resulting in a greatly increased recombination activity.

(b) Passivation, presumably with hydrogen, may be a good alternative for reducing the recombination activity of $FeSi_2$ clusters. There is already evidence that iron clusters can be rendered recombination-inactive as the result of hydrogen passivation [12], although many properties of this reaction are poorly understood and warrant additional investigation.

(c) By restricting the dissolution of foreign particles within the melt, it is perhaps possible to limit the dissolved Fe concentration within the melt, and thus the abundance of resulting Type 1 particles. This may be achieved by reducing the time the feedstock remains in liquid form, while ensuring that large second-phase particles become included into the crystal rather than segregated from it. Unfortunately, for block cast mc-Si, the feedstock remains in liquid form in contact with the crucible for a considerable length of time, as long as several hours, and the growth speed is rather slow, several microns/s. Novel methods, such as electromagnetic casting, reduce considerably the time the feedstock is in liquid form, by increasing the pull rate and reducing the size of the molten zone. In addition, the increased pull rate allows for larger second-phase particles to be incorporated wholly into the forming crystal. It is thus not surprising that in mc-Si grown by this technique, large (12 - 30+ µm in diameter) oxidized Fe particle clusters were identified via µ-XRF/XAS by McHugo *et al.* [5]. Also, LBIC measurements by Périchaud *et al.* [8] have indicated that aside from isolated regions of recombination activity at metallic inclusions, the recombination activity of most structural defects is rather low at room temperature, in contrast to recombination-active structural defects in block cast mc-Si. The drawback of EMCP is that faster pull rates produce lower effective segregation coefficients for Fe, resulting in a greater point defect concentration. Thus, a gettering or passivaiton step is required, with temperatures low enough as not to significantly dissolve the metallic inclusions.

5 CONCLUSIONS

Synchrotron-based microprobe techniques have been applied to investigate the distribution, size, chemical state, and recombination activity of Fe-rich clusters in two mc-Si materials: sheet material and cast mc-Si. In the former, a high concentration ($\sim 2\times10^7$ cm^{-2}) of rather large (23±5 nm radius) iron silicide particles were observed along the grain boundary. Metals were also found concentrated at intragranular clusters, which in as-grown material have a composition similar to stainless steel. It is believed that these clusters, likely introduced into the melt from the feedstock, rapidly dissolve during crystal growth and during high-temperature device processing, leading to the contamination of nearby structural defects such as grain boundaries, and to the formation of smaller Fe silicide particles. Materials improvements can be expected by increasing grain size near the pn junction, reducing the density of intragranular metallic clusters near the pn junction, and by retarding the dissolution of these foreign particles in the feestock, perhaps by oxidizing them. In cast mc-Si, two types of clusters were observed: Type 1, consisting of sub-micron $FeSi_2$ particles elongated along the crystal growth direction, and Type 2, consisting of micron-sized

Fe_2O_3 particles, containing as well detectable quantities of other metals (Cr, Mn, Ti, Ca), not preferentially oriented in the direction of crystal growth. It is believed that Type 2 particles, because of their size and oxidized state, are inclusions formed of foreign, second-phase particles. Because it is known that oxidized iron is attacked and reduced by liquid silicon, it is suspected that these Type 2 particles are the source of Fe for the smaller, more distributed, and more dangerous Type 1 particles. In light of this information on the nature and distribution of Fe clusters in silicon, these possible solutions for reducing the negative impact of Fe contamination in mc-Si are discussed: gettering, passivation, and inhibiting the dissolution of foreign particles within the melt.

6 ACKNOWLEDGEMENTS

This work was funded by NREL subcontract AAT-2-31605-03, and the AG-Solar project of the government of Northrhein-Westfalia (NRW), funded through the Fraunhofer Institute for Solar Energy Systems (ISE) (Germany). M. Heuer thanks the Deutsche Forschungsgemeinschaft for funding the project HE 3570/1-1. The operations of the Advanced Light Source and Advanced Photon Source are supported by the Director, Office of Basic Energy Sciences of the U.S. Department of Energy under Contract No. DE-AC03-76SF00098 and W-31-109-ENG-38, respectively.

7 REFERNECES

[1] D. Macdonald, A. Cuevas, A. Kinomura, Y. Nakano, in *29th IEEE PVSC*, New Orleans, USA, (2002).
[2] A. A. Istratov, T. Buonassisi, R. J. McDonald, et al., J. Appl. Phys. **94**, 6552 (2003).
[3] A. A. Istratov, H. Hieslmair, and E. R. Weber, Appl. Phys. A **70**, 489 (2000).
[4] T. Buonassisi, O. F. Vyvenko, A. A. Istratov, et al., Physica B **340-342**, 1137 (2003).
[5] S. A. McHugo, A. C. Thompson, A. Mohammed, et al., J. Appl. Phys. **89**, 4282 (2001).
[6] S. A. McHugo, A. C. Thompson, C. Flink, et al., J. Cryst. Growth **210**, 395 (2000).
[7] P. S. Plekhanov, R. Gafiteanu, U. M. Gosele, and T. Y. Tan, J. Appl. Phys. **86**, 2453 (1999).
[8] I. Périchaud, S. Martinuzzi, and F. Durand, Solar Energy Mater. & Solar Cells **72**, 101 (2002).
[9] J.Isenberg, W.Warta, J. Appl. Phys. **95**,5200 (2004).
[10] A. Fedotov, B. Evtody, L. Fionova, et al., J. Cryst. Growth **104**, 186 (1990).
[11] S. A. McHugo, H. Hieslmair, and E. R. Weber, Appl. Phys. A **64**, 127 (1997).
[12] O. F. Vyvenko, T. Buonassisi, A. A. Istratov, et al., J. Phys: Cond. Matter **14**, 13079 (2002).
[13] M. Rinio, D. Borchert, et al., Proc. 19th European Photovoltaic Solar Energy Conference (2004).
[14] J. Lu, M. Wagener, G. Rozgonyi, et al., J. Appl. Phys. **94**, 140 (2003).
[15] M. A. Marcus, A. A. MacDowell, R. Celestre et al., J. Synchrotron Rad. **11**, 239 (2004).
[16] Z. Cai, B. Lai, W. Yun, et al., AIP Conference Proceeedings **521**, 31 (2000).

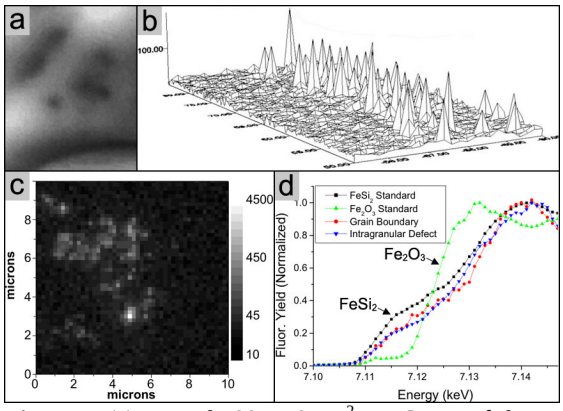

Figure 1: (a) Typical 100×150 μm^2 XBIC map of sheet material, showing a grain boundary and localized intragranular defects. Lower XBIC signal is dark. (b) 35×5 μm^2 µ-XRF map of Fe nanoprecipitates at the grain boundary. (c) µ-XRF map of sub-micron Fe distribution within an intragranular defect. Note log scale of Fe concentration (a.u.). (d) µ-XAS reveals the chemical state matches best with $FeSi_2$, not Fe_2O_3.

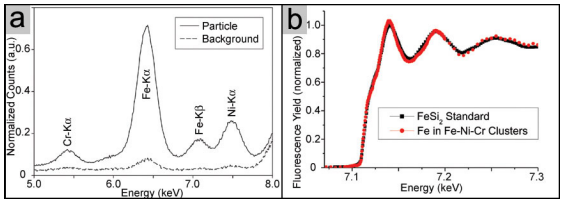

Figure 2: (a) µ-XRF point spectrum of a Cr-Ni-Fe-rich particle in as-grown sheet material. The relative heights of the peaks suggest stainless steel. (b) µ-XAS unambiguously indicates Fe is present as $FeSi_2$.

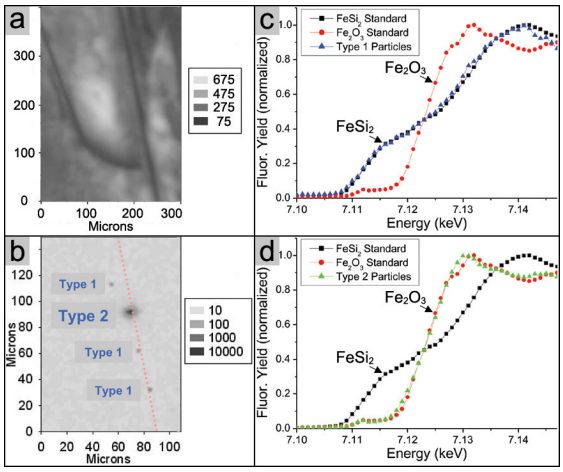

Figure 3: (a) Typical XBIC (a.u.) of a sample from the bottom region of a block cast mc-Si ingot showing a recombination active grain boundary. Positive contrast (higher XBIC signal is white). (b) µ-XRF map along a portion of the grain boundary, showing 4 Fe clusters. Dotted line indicates the grain boundary location. Note log scale of Fe concentration (a.u.). (c) Average µ-XAS spectrum from 4 Type 1 clusters matches well with $FeSi_2$. (d) Average µ-XAS spectrum from 2 Type 2 clusters matches well with Fe_2O_3.